Langmuir
Letter
pubs.acs.org/Langmuir

Dynamic Imaging of Colloidal-Crystal Nanostructures at 200 Frames per Second

Marcel A. Lauterbach, Chaitanya K. Ullal,* Volker Westphal, and Stefan W. Hell*

Max Planck Institute for Biophysical Chemistry, Am Fassberg 11, 37075 Göttingen, Germany

Received June 17, 2010. Revised Manuscript Received August 3, 2010

The dynamic noninvasive imaging of colloidal nanostructures has been precluded by the diffraction-limited resolution of (confocal) light microscopy. Using Fast Stimulated Emission Depletion (STED) microscopy, we demonstrate the ability to resolve the formation of a colloidal crystal (monolayer) from particles of 200 nm size, where the voids in the crystal are as small as 30 nm. With a temporal resolution of 5 ms, we exemplify the technique by visualizing the annealing of potential point defects during the formation of the colloidal crystal.

Introduction

Colloidal particles can assemble into crystals, which are important model systems for atomic and ionic crystals. They have been used to determine the Avogadro number, study glass transitions, and analyze nucleation and crystal growth, as well as build photonic crystals.[1]

Confocal microscopy has contributed significantly to the study of these model colloidal systems,[2] the simplest of which consists of a monodisperse suspension of "hard" spheres that do not interact for separations greater than their diameter. The introduction of complex attractive and repulsive forces that are more representative of the bonds between atoms results in a richer diversity of structures.[3−6] The basic interactions of larger particles are fairly well understood. However, the extension of this knowledge to the nanoscale by simply changing the dimensions of the particles, while valid in some cases, is not generally established.[7] The experimental observation of such phases as diamond-like crystals[4] and the enhanced properties of nanostructures due to their constituent particle sizes[8] provide strong motivation to study colloidal crystals at the nanoscale.

The primary advantage of confocal microscopy is the ease with which in situ, real-space, real-time images can be recorded noninvasively. Unfortunately, the resolution of a confocal microscope is limited by the diffraction barrier. The study of model colloidal nanostructures would thus greatly benefit from the implementation of an imaging scheme that affords subdiffraction resolution while retaining the benefits of confocal microscopy. Far-field fluorescence nanoscopes[9] have the ability to image with resolutions far beyond the diffraction barrier. Their successful imaging of three-dimensional[10,11] and dynamic (biological) systems[12,13] makes them obvious candidates in this regard. STED microscopy,[14,15] the first nanoscopy method to be conceived and demonstrated, has been applied to the imaging of dense 3D colloidal nanostructures,[10] as well as the visualization of diffusing colloidal particles.[12]

A common implementation of the STED microscope is as a laser scanning microscope: Fluorescence is elicited by a focused laser beam and detected point by point. In STED microscopy, the fluorescence ability of the fluorophores in the outer part of the excitation focus is transiently turned off. This generates a smaller effective excitation volume. The switching of the molecules into a nonfluorescent state is achieved via stimulated emission with a second, red-shifted, laser beam ("STED beam"). A STED focus of toroidal ("donut") shape is overlaid onto the excitation focus (Figure 1A). Thus, the ability of the fluorophores to emit is turned off via stimulated emission in the periphery of the excitation focus. Only at the very center, where the STED focus has close-to-zero intensity, are the fluorophores able to spend significant time in the fluorescent state. The area wherein the fluorophores are not switched off, and accordingly the minimally resolvable distance, shrinks to zero with increasing intensity of the STED beam.

In this paper, we demonstrate the ability of STED microscopy to image the dynamics of dense colloidal crystals with subdiffraction resolution. The Fast STED microscope, which incorporates a resonant beam scanner operating at 15.8 kHz, bidirectional scanning along both lateral axes with sinusoidal speed profiles, a fast photodetector, and fast data acquisition with a field programmable gate array, allows us to image at frame rates as high as 200 frames per second (fps).

We exemplify the relevance of such a system to colloidal nanostructures by the in situ recording of movies in colloidal crystals as they form by convective assembly. This involves the

*To whom correspondence should be addressed. E-mail: ckullal@alum.mit.edu; shell@gwdg.de. Phone: +49 (0)551 201 2510; +49 (0)551 201 2500. Fax: +49 (0)551 201 2505; +49 (0)551 201 2505.

(1) Gasser, U. *J. Phys.: Condens. Matter* **2009**, *21*, 203101.
(2) Prasad, V.; Semwogerere, D.; Weeks, E. R. *J. Phys.: Condens. Matter* **2007**, *19*, 113102.
(3) Glotzer, S. C.; Solomon, M. J. *Nat. Mater.* **2007**, *6*, 557–562.
(4) Kalsin, A. M.; Fialkowski, M.; Paszewski, M.; Smoukov, S. K.; Bishop, K. J. M.; Grzybowski, B. A. *Science* **2006**, *312*, 420–424.
(5) Shevchenko, E. V.; Talapin, D. V.; Kotov, N. A.; O'Brien, S.; Murray, C. B. *Nature* **2006**, *439*, 55–59.
(6) Leunissen, M. E.; Christova, C. G.; Hynninen, A.-P.; Royall, C. P.; Campbell, A. I.; Imhof, A.; Dijkstra, M.; van Roij, R.; van Blaaderen, A. *Nature* **2005**, *437*, 235–240.
(7) Bishop, K. J. M.; Wilmer, C. E.; Soh, S.; Grzybowski, B. A. *Small* **2009**, *5*, 1600–1630.
(8) Urban, J. J.; Talapin, D. V.; Shevchenko, E. V.; Kagan, C. R.; Murray, C. B. *Nat. Mater.* **2007**, *6*, 115–121.
(9) Hell, S. W. *Science* **2007**, *316*, 1153–1158.
(10) Harke, B.; Ullal, C. K.; Keller, J.; Hell, S. W. *Nano Lett.* **2008**, *8*, 1309–1313.
(11) Schmidt, R.; Wurm, C. A.; Jakobs, S.; Engelhardt, J.; Egner, A.; Hell, S. W. *Nat. Methods* **2008**, *5*, 539–544.
(12) Westphal, V.; Lauterbach, M. A.; Di Nicola, A.; Hell, S. W. *New J. Phys.* **2007**, *9*, 435.
(13) Westphal, V.; Rizzoli, S. O.; Lauterbach, M. A.; Kamin, D.; Jahn, R.; Hell, S. W. *Science* **2008**, *320*, 246–249.
(14) Hell, S. W.; Wichmann, J. *Opt. Lett.* **1994**, *19*, 780–782.
(15) Klar, T. A.; Hell, S. W. *Opt. Lett.* **1999**, *24*, 954–956.

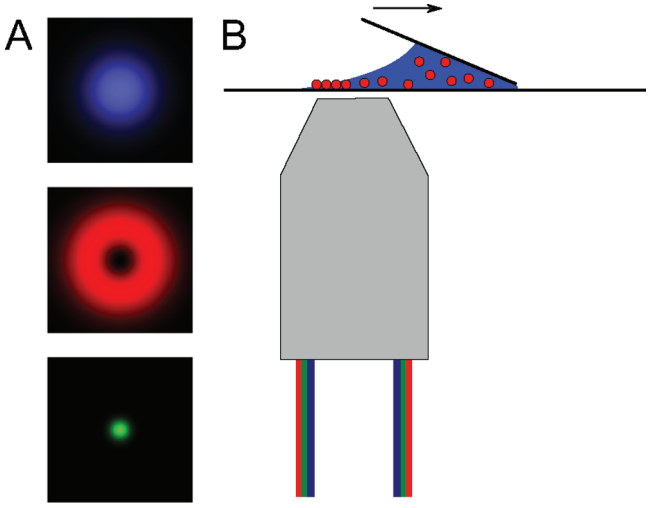

Figure 1. (A) Foci used for STED microscopy: Overlaying the regularly focused excitation focus (upper panel) with a toroidal STED focus (center panel) leads to a very small area in which the fluorescent state of the fluorophore can be populated (lower panel). (B) Sample configuration to form colloidal monolayers in the microscope. The meniscus of a drop of bead suspension (blue) is observed through a coverslip (black) in the inverted microscope. The whole drop shifts, if the second, tilted coverslip (black), to which it adheres, is moved to the right. The colloidal monolayer of nanoparticles (red) forms at the meniscus.

self-organization of colloidal particles from a suspension via the controlled evaporation of the solvent at a moving contact line.[16] The particles are brought to the crystal growth front by the flow of the solvent compensating for the evaporation from the crystal surface. The morphology of the resultant colloidal crystal is known to depend on various factors such as the volume fraction of the particles in the suspension and the flux of solvent compensating for the evaporation.[17] The high speed of the Fast STED microscope allowed us to observe the annealing of potential point defects during the formation of the crystal.

Methods

STED Microscopy. We employed a home-built one-axis beam-scanning STED microscope.[12] A resonant beam scanner (SC-30, EOPC, Glendale, NY, USA), operating at 15.8 kHz, was used for one-axis beam steering. For the second lateral axis, stage-scanning was implemented. Both axes were scanned bidirectionally, i.e., the flyback was used for data acquisition, too. For fast scanning, on both axes a sinusoidal speed profile was employed. This allowed us to record up to 31 600 lines per second. Thus, a frame rate of 200 fps was achieved at an image size of (1.8×1.5) μm^2. Due to the sinusoidal movement of the resonant scanner, corrections to the image brightness and dwell times were necessary. To this end, the primary data were collected with a pixel dwell time that was maximally half of the dwell time in the final image. The brightness and pixel sizes were then corrected for the sinusoidal movement of the scanner. A custom-built field-programmable gate array board allowed for fast photon counting and data preprocessing.

A fiber-coupled counting photomultiplier (PMT) (H7422PA-40 select, Hamamatsu, Herrsching am Ammersee, Germany) was used for fluorescence detection. The PMT has the advantage of a large dynamic range; ~1100 counts per frame were recorded from each bead; the background amounted on the same area to only ~15 counts. To use the fastest digitizing possible, the output of the PMT was digitized with 1 bit depth (i.e., high/low) every 5 ns, corresponding to the pulse width of the PMT used.

The excitation beam (635 nm) had in the aperture of the objective (NA = 1.4, oil immersion, HCX PL AP, Leica, Heidelberg, Germany) a power of 15 μW during the STED recordings and of 1.9 μW during confocal recordings. The STED beam (750 nm) had a power of 43 mW in the aperture of the objective.

Formation of Colloidal Crystals under the Microscope. Convective assembly was used to form colloidal crystals under the microscope. A drop of colloidal suspension was moved over a coverslip (Figure 1B). A large coverslip [(22×60) mm^2] through which the sample was observed was glued to an aluminum frame. A second, smaller coverslip [(10×20) mm^2] was mounted at an angle of ~30° above it. The small coverslip could be moved laterally with a piezo motor (Piezo LEGS Linear 10 N, Piezo-Motor, Uppsala AB, Uppsala, Sweden). The gap between the two coverslips was ~0.2 mm. The corner between the two coverslips was filled with a suspension of fluorescent 200 nm polystyrene beads [Crimson, Invitrogen, 2% (w/v)]. The formation of colloidal crystals was observed at the free (rear) end of the drop with an inverted microscope.

Cleaning of the Coverslips. Coverslips were first submerged in acetone, then in methanol. The remaining methanol was blown off. The coverslip surfaces were then cleaned and made hydrophilic in a plasma cleaner (15 min, process gas air at (0.2−1) hPa, radio frequency 13.56 MHz, ~60 W, FEMTO, Diener Electronic, Nagold, Germany).

Deconvolution. Images were linearly deconvolved (Wiener filtering) using a two-dimensional Lorentz function of 60 nm FWHM as a kernel.

Results and Discussion

We used a specific implementation of convective assembly known as confined convective assembly[18] to form colloidal crystals. This involves dragging a drop of the colloidal suspension, confined in a meniscus between two glass slides, at a constant velocity across the surface of one of the slides (Figure 1B). The use of confined convective assembly over regular convective assembly reduces the volume of the suspension required and, importantly, dramatically increases the speed of deposition. Crystal growth rates in the case of confined convective assembly are typically on the order of tens of micrometers per second. This puts an exacting technical requirement on the associated imaging process.

We targeted deposition conditions that resulted in the formation of a monolayer of the colloidal crystals. Figure 2 shows a direct comparison of the confocal and STED images of the resultant crystal consisting of 200 nm beads arranged on a two-dimensional hexagonal close-packed lattice. The figure clearly demonstrates that only STED microscopy is able to resolve the individual particles in the colloidal crystal. The structure of the monolayer is clearly visualized in the Fast-STED-microscopy image despite the fact that the voids between the 200 nm spheres are only 30 nm in diameter. If desired, linear deconvolution can be employed to make the beads even more clearly visible (right). In contrast, deconvolution of the confocal image simply emphasizes the noise present in the image. It is important to note that the use of commercially available monodisperse 200 nm beads does not represent a limit on the capability of the STED microscope. The resolution of the STED microscope has an inverse square root dependence on the intensity of the STED beam; in theory, there is no lower bound on the resolution.[19]

(16) Denkov, N. D.; Velev, O. D.; Kralchevsky, P. A.; Ivanov, I. B.; Yoshimura, H.; Nagayama, K. *Langmuir* **1992**, *8*, 3183–3190.
(17) Norris, D. J.; Arlinghaus, E. G.; Meng, L.; Heiny, R.; Scriven, L. E. *Adv. Mater.* **2004**, *16*, 1393–1399.
(18) Prevo, B. G.; Velev, O. D. *Langmuir* **2004**, *20*, 2099–2107.
(19) Harke, B.; Keller, J.; Ullal, C. K.; Westphal, V.; Schönle, A.; Hell, S. W. *Opt. Express* **2008**, *16*, 4154–4162.

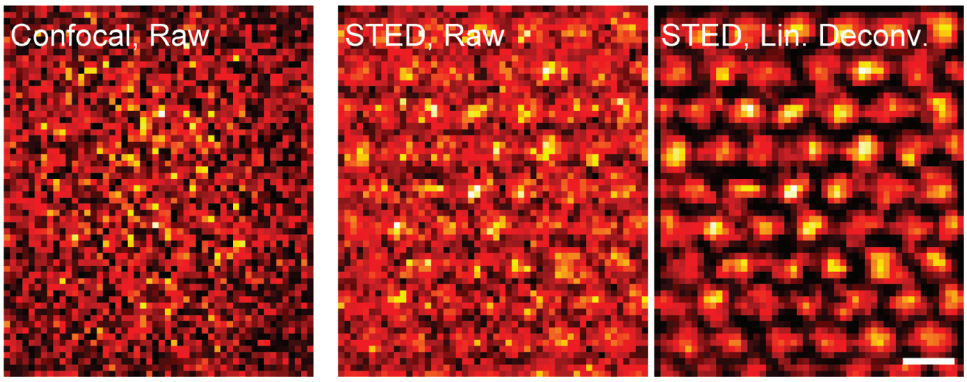

Figure 2. Comparison of confocal and STED images of a colloidal monolayer. Left: confocal image, the individual particles are not resolved. Middle: STED image, the individual particles are resolved. Right: STED image after linear deconvolution, the individual particles can be discerned very clearly. Scale bar 250 nm.

Under our experimental conditions, the colloidal-crystal monolayers were formed when the contact line of the suspension on the glass was moved at a speed of 34 μm/s (Figure 3 and Supporting Information movie S1). The crystal growth was recorded as a movie at 200 fps via Fast STED microscopy. Figure 3 shows still frames taken from a representative movie as the growth front sweeps across the imaged area. Colloidal particles are transported from the bulk suspension to the crystal growth front by the solvent and into the voids along the front. The solvent itself flows on through the connected voids of the deposited crystal to the many small menisci in these voids, to finally evaporate from the exposed surface of the deposited crystal. The exact mechanism by which convective assembly forms 3D colloidal crystals is still the subject of research.[17] Although our system is restricted to observing the formation of a monolayer, the images we obtain seem to be in keeping with the convective steering hypothesis.[17,20] Imaging the rapidly moving crystal front exemplifies our ability to reveal details of the growth process. For example, we observed the elimination of a potential defect. The particle marked with a white arrow in Figure 3 does not occupy the void in front of it until its neighbor, which is identified by the blue arrowheads and already touching the growth front, has moved from its incorrect position to the correct lattice point in the growing crystal.

Having imaged the dynamics associated with dense colloidal crystals at resolutions that are inaccessible to confocal microscopy, it is useful to examine the relative merits of our particular implementation: All currently known microscopy techniques that break the diffraction barrier, including those based on single molecule switching with stochastic readout,[21] do so by time-sequential readout of nanoscale information from each diffraction-limited volume or area. Despite this commonality, methods that rely on stochastic readout cannot currently achieve the imaging speeds demonstrated in this paper. The reason for this is twofold. First, the stochastic methods are hampered by the current state of technology: the frame rates of the cameras are relatively low and the available dyes show a suboptimal blinking behavior. Relying on stochastic readout to create images with enough detail to outline the colloidal particles would require 10 000−100 000 individual frames. At 1000 fps, the assembly of a single image would thus take (10−100) s; during this time, the colloidal particles move a distance far more than their diameter, thereby precluding high-resolution imaging.

Second, and more importantly, targeted switching methods such as STED microscopy have a fundamental advantage from the perspective of labeling density. Generally, only a threshold number of photons needs to be registered from each object in order to distinguish it from the background. The denser the labeling, the faster these photons can be collected and the scanning performed. The imaging speed in STED microscopy therefore scales with the labeling density of the features of interest. This is in contrast to stochastic switching methods where in each frame not more than one marker molecule can be registered per diffraction limited zone regardless of the labeling density. Furthermore, a smaller field of view (FOV) translates in STED microscopy directly into higher frame rates, whereas in the stochastic scanning methods, the frame rate is independent of the FOV.

Summary and Conclusions

The formation of dense colloidal crystals, whose voids are as small as 30 nm, by particles 200 nm in diameter was imaged for the first time via Fast STED microscopy. The deposition of a monolayer during confined convective assembly was filmed at 200 fps, i.e., at 8 times the video rate (Figure 3), a speed that has never been reached in this context before. Fast STED microscopy could resolve details of the processes at the growth front. In particular, the arrival of a particle at the growth front and its subsequent incorporation, predicated by the elimination of a previous defect in the crystal lattice, was visualized (Figure 3).

Although the study of colloidal crystals has benefited tremendously from the use of confocal microscopy, it had always been limited to the relatively slow movement of micrometer-sized particles, thereby precluding the study of dynamics in colloidal nanostructures. A direct comparison with confocal microscopy showed that the crystal structure of the nanostructured monolayer can only be resolved via STED microscopy (Figure 2).

The experiments presented here serve as a signpost for the subdiffraction resolution imaging of dynamics in dense colloidal crystals. Emphasis will now be on combining two primary advantages of far-field fluorescence imaging for colloidal studies: Dynamic and three-dimensional imaging. The essential elements for three-dimensional high-resolution imaging have recently been demonstrated; increased axial resolution is possible through the simultaneous use of either multiple depletion patterns[10] or coherently opposed lenses.[11] The STED microscope employed here operates with a single focus only. In a parallelized version,[9] each

(20) Gasperino, D.; Meng, L.; Norris, D. J.; Derby, J. J. *J. Cryst. Growth* **2008**, *310*, 131–139.
(21) Huang, B.; Bates, M.; Zhuang, X. *Annu. Rev. Biochem.* **2009**, *78*, 993–1016.

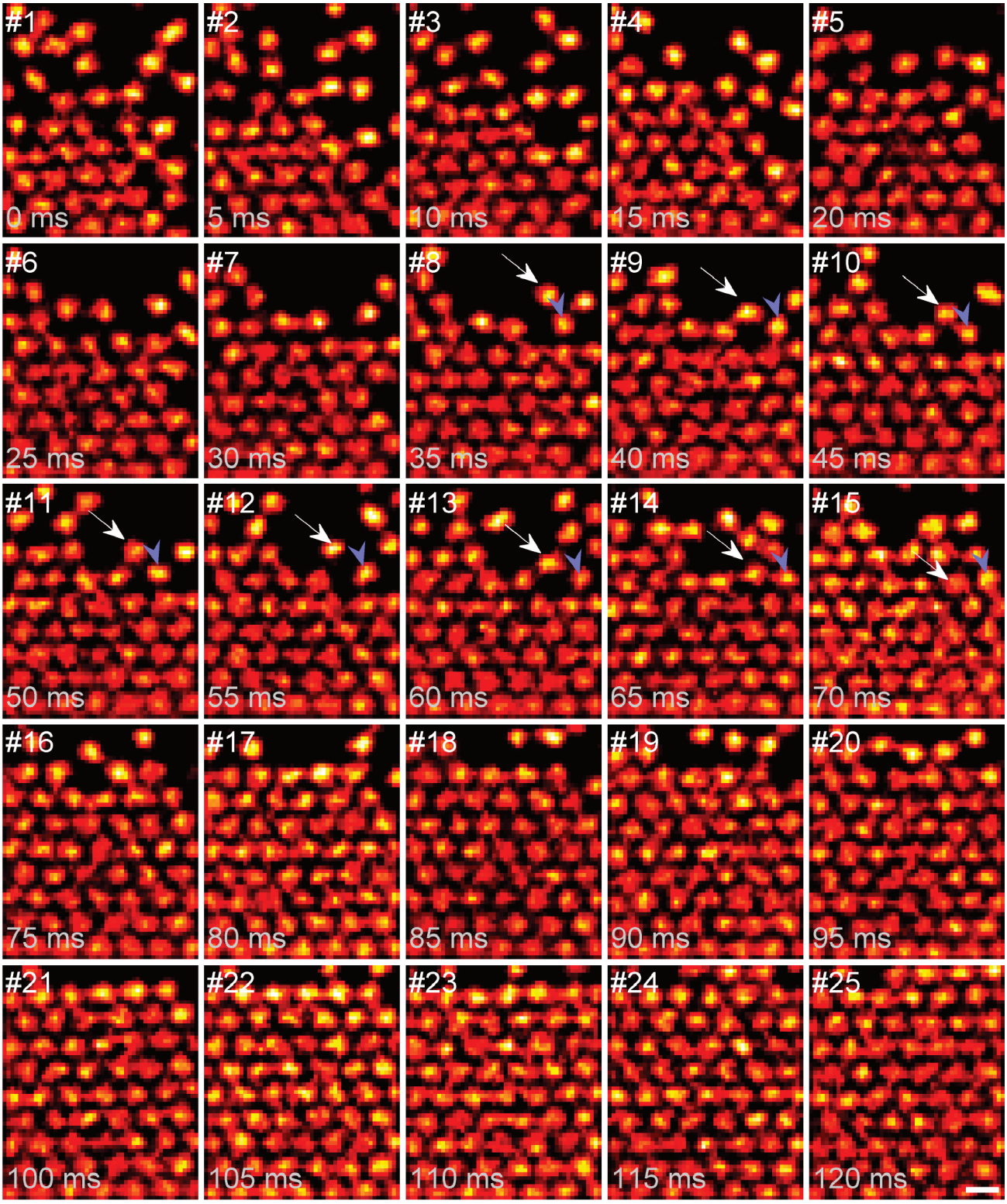

Figure 3. Formation of a colloidal crystal. Successive movie frames of a colloidal crystal (monolayer), which is just forming. The movie is recorded at 200 fps and available online (Supporting Information movie S1). Two particles are highlighted in several frames by white arrows and blue arrowheads, respectively. Note how the bead marked with the blue arrow heads blocks in frames 10−12 the lattice site for the newly arriving bead marked with the white arrows. Data shown after linear deconvolution. Scale bar 250 nm.

diffraction limited area could be scanned by its own focus with the potential to increase the speed. Alternatively, the FOV could be extended without penalty if more foci were to be employed. It is important to notice that for observing colloidal crystal formation only the surface/growth front needs to be scanned repeatedly, not the whole (static) crystal volume. The demands on additional scanning speed for 3D imaging are thus moderate. In conclusion, the work presented in this paper opens the door to studies of

colloidal nanoparticles with their associated faster dynamics and their assembly into crystals.

Acknowledgment. We thank Andreas Schönle for helpful discussions and suggestions on the manuscript and for his Software Imspector. C.K.U. acknowledges a fellowship of the Max Planck Society. M.A.L. was supported by the German National Academic Foundation. This work was supported by the Leibniz Prize of the Deutsche Forschungsgemeinschaft to S.W.H.

Supporting Information Available: Full Movie S1 of the colloidal-crystal formation, of which some frames are shown in Figure 3. This material is available free of charge via the Internet at http://pubs.acs.org.